ACS Sustainable Chemistry & Engineering

Research Article

pubs.acs.org/journal/ascecg

Molecular Characterization of Extracts from Biorefinery Wastes and Evaluation of Their Plant Biostimulation

Davide Savy,*[,†,‡] Pierluigi Mazzei,[†] Marios Drosos,[†] Vincenza Cozzolino,[†,‡] Licia Lama,[§] and Alessandro Piccolo*[,†,‡]

[†]Centro Interdipartimentale di Ricerca sulla Risonanza Magnetica Nucleare per l'Ambiente, l'Agro-Alimentare ed i Nuovi Materiali (CERMANU), and [‡]Dipartimento di Agraria, Università di Napoli Federico II, Via Università 100, 80055 Portici, Italy

[§]CNR—National Research Council of Italy, Institute of Biomolecular Chemistry, Via Campi Flegrei 34, 80078 Pozzuoli, Italy

Supporting Information

ABSTRACT: Biorefinery residues from non-food biomasses are promising sources of sustainable agrochemicals. The molecular properties of water-soluble extracts from ligno-cellulosic biomass pretreated first by steam-explosion and then by enzymatic hydrolyses at different buffer doses, were assayed for bioactivity on maize. ^{13}C and ^{31}P nuclear magnetic resonance (NMR) spectra showed that extracts varied in phenolic and carboxyl content, while high performance size exclusion chromatography and diffusion ordered spectroscopy NMR revealed that Ox-BYP 1 obtained from wastes treated with a greater buffer dose contained small-sized molecules associated in apparently large metastable aggregates. Ox-BYP 2 separated from wastes treated with smaller buffer concentrations showed a more stable conformation. Both hydrolysates revealed a positive dose-dependent bioactivity toward maize growth. Ox-BYP 1 promoted plant fresh and dry weights and root length at 10 and 100 ppm but decreased seedling growth at 1 ppm. Instead, Ox-BYP 2 increased the whole plant growth at all assayed concentrations. Their different biostimulation effects were attributed to the toxicity of easily bioaccessible lignin-derived phenolics at small concentrations of Ox-BYP 1, which was removed by molecular self-assembly at greater concentrations. Conversely, the more strongly associated Ox-BYP 2 exerted a positive bioactivity even at small doses. The bioactivity of extracts from biorefinery wastes appeared to depend on molecular composition and, in turn, on waste pretreatments.

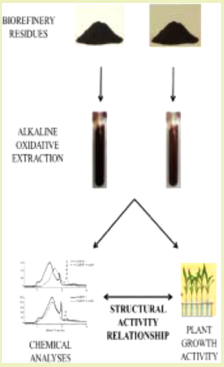

KEYWORDS: *Biorefinery residues, Plant biostimulants, Water-soluble extracts, Humic-like materials, ^{13}C—CPMAS NMR, ^{31}P NMR, ^{1}H-DOSY NMR, HPSEC, 2-Chloro-4,4,5,5-tetramethyl-1,3,2-dioxa-phospholane*

INTRODUCTION

Fossil fuel exploitation is one of the major causes of greenhouse gas emissions, global warming, biodiversity losses, and negative impacts on plant growth and development.[1,2] Since actual fossil fuel reserves are estimated to be exhausted within the next 40—50 years,[3] a sustainable alternative is the production of ethanol for energy from cellulose-rich *non*food biomasses, agricultural residues, or biogenic wastes.[4] Moreover, the photosynthates isolated from plant cells are progressively used to produce various chemicals and alleviate industrial dependence on fossil-derived commodities.[5] Biorefinery processes are often fueled by lignin-rich residues,[6] despite the inherent photosynthate value of lignin.[7,8] In fact, a novel added-value to biorefineries is conferred by lignin byproducts employed as adhesives, polymers, and blends,[9] thereby contributing to industry sustainability.[10,11] Lignin-rich residues were also found to be suitable as soil conditioners or plant biostimulants in order to increase the sustainable productivity of agricultural crops.[12,13]

Water-soluble humic-like biostimulants have been isolated from *non*food lignocellulosic biomasses by an alkaline H_2O_2 extraction.[14] This treatment efficiently breaks down the lignin cell polymer, whose small oxidized humic-like molecules are easily solubilized.[15] The water-soluble fragmented lignin was separated from different lignocellulosic biomasses and showed a positive, hormetic bioactivity toward the emergence of maize (*Zea mays* L.) seeds and early growth of seedlings.[13,16] For instance, humic-like water lignins from cardoon (*Cynara cardunculus* L) stimulated the coleoptile length of maize seeds up to 72% more than control, while those from miscanthus (*Miscanthus χ Giganteus* Greef et Deuter) biomass enhanced the lateral seminal root elongation by 74% more than control, and those from giant reed (*Arundo donax* L.) biomass promoted shoot and root dry weight of maize seedlings up to 50% and 33% more than control, respectively.[13,16]

Water-soluble plant biostimulants are currently isolated from different sources such as composted biomasses,[17,18] seaweeds,[19] or agro-industrial residues.[20,21] To our knowledge, plant biostimulants from lignin-rich biorefinery wastes remaining after separation of cellulose for conversion into industrial products have never been isolated. The aim of this work was to extract water-soluble biostimulants by an oxidative alkaline solution from two lignocellulosic residues remaining after steam

Received: June 14, 2017
Revised: July 14, 2017
Published: August 31, 2017

DOI: 10.1021/acssuschemeng.7b01928
ACS Sustainable Chem. Eng. XXXX, XXX, XXX—XXX

explosion and hydrolysis, structurally characterize the extracts, and evaluate their biological activity on germination of maize seeds and growth of maize plantlets.

MATERIALS AND METHODS

Biomasses. Giant reed (*Arundo donax* L.—GR) is an interesting biomass for biorefineries because of the large dry biomass yield per hectare, the capacity of growing on different soils without significant yield variation, the resistance to both biotic and abiotic adversities, and the minimum attention required for its growth.[22,23] GR stems and leaves were pretreated by steam-explosion according to the work of Garbero et al.[24] and De Bari et al.[25] The resulting byproduct was then subjected to two different procedures of enzymatic hydrolysis with the aim to increase cellulose bioavailability. The bioconversion mixture consisted of 1 L sodium acetate buffer at pH 5.2/kg of wet lignocellulosic biomass. The final concentration of the applied sodium acetate buffer was either 100 mM for an incubation period of 72 h or 50 mM of for 48 h, yielding the BYP 1 and BYP 2 hydrolysates, respectively. The hydrolysis was carried out in Biostat 50 L bioreactor (B. Braun Biotech International, Germany) at 45 °C at 100 rpm, using the commercial enzymatic cocktail Novozymes NS22201 according to the work of Cimini et al.[26] After bioconversion, the solid BYP 1 and BYP 2 residues were recovered with a peristaltic pump to separate them from the supernatant, which has been further microbially treated to obtain succinic acid. The solid residues were extensively washed with deionized water until ion-free and stored before further treatment at −20 °C.

Extraction by Alkaline Oxidative Hydrolysis. An aliquot (10.0 g) of both residues was added with 300 mL of a 2% H_2O_2 (v/v) aqueous solution at a pH brought to 11.5 with a 4 M KOH solution. After stirring overnight at 50 °C, the mixture was centrifuged (15 400 RCF × 20 min) and the supernatant dialyzed (1 kDa cutoff dialysis tubes) against deionized water, freeze-dried, and stored in dried conditions for further analyses. The water-soluble extracts separated from BYP 1 and BYP 2 were labeled as Ox-BYP 1 and Ox-BYP 2, respectively.

Elemental Analysis. The elemental composition of both BYP and Ox-BYP substrates was determined by an EA 1108 elemental analyzer (Fisons Instruments). The ash content was measured as by the ASTM E1755-01 standard method.[27]

Synthesis of 2-Chloro-4,4,5,5-Tetramethyldioxaphospholane. The derivatizing phosphorus reagent 2-chloro-4,4,5,5-tetramethyldioxaphospholane (CTMP) was synthesized as described elsewhere.[28] Briefly, CTMP was obtained by mixing the two following solutions: solution A, prepared by dissolving 21.5 mL PCl_3 in 180 mL of dry *n*-hexane placed in a 250 mL three-necked round flask equipped with a condenser, and solution B, prepared by dissolving 23.7 g pinacol in a mixture of 32 mL of dry pyridine and 150 mL of dry *n*-hexane placed in a conic flask. Solution B was added dropwise to solution A using an addition funnel placed on the second neck of the round flask. The addition lasted 1 h under vigorous stirring in an ice bath, then the mixture was left for 1 h at room temperature to complete the reaction. The solution was filtered on a filter paper, while the whitish residue on the filter was rinsed with 2 × 100 mL of *n*-hexane and the filtrates were evaporated under *vacuum* at 328 K. Finally, CTMP was separated from solution by *vacuum* distillation (bp 97 °C at 4 mbar).

Extract Derivatization Prior to ^{31}P NMR Spectroscopy. The hydroxyl (OH) groups in the lignin-rich Ox-extracts were derivatized with CTMP, in order to obtain a quantitative evaluation by ^{31}P nuclear magnetic resonance (NMR) spectra. A stock solution was made by adding to a pyridine and deuterated chloroform solution (1.6/1 v/v), 2.92 mg mL^{-1} cyclohexanol as internal standard, 10.0 mg mL^{-1} of triphenyl phosphate as reference peak for the ^{31}P frequency axis calibration and 0.6 mg mL^{-1} of chromium(III) acetylacetonate as relaxation agent. The Ox-extracts (7.0 mg) were dissolved in 750 μL of the stock solution and added with 50 μL of the previously synthesized CTMP as ^{31}P derivatization agents. The NMR tube was ultrasonicated for 1 min prior to loading into the NMR magnet.

NMR Spectroscopy. The solid-state ^{13}C cross-polarization magic angle spinning (CPMAS) NMR spectra were acquired with a 300 MHz wide-bore Bruker Avance magnet (Bruker Bio Spin GmbH, Rheinstetten, Germany), equipped with a CPMAS probe, working at ^{13}C frequency of 75.47 MHz. Samples were loaded into 4 mm zirconia rotors, closed with Kel-F caps and spun at a rate of 10000 ± 1 Hz. Such spectra were acquired by applying a cross-polarization technique and consisted of 1814 time domain points, a spectral width of 300 ppm (22 727.3 Hz), a recycle delay of 2 s, 5000 scans, and 1 ms of contact time. The ^{13}C CPMAS pulse sequence was conducted by using a ^{1}H ramp pulse to account for the *non*homogeneity of the Hartmann—Hahn condition. A TPPM15 scheme was applied to perform the ^{13}C—^{1}H decoupling. The free induction decay (FID) was transformed by applying a 4k zero filling and an exponential filter function with line broadening of 100 Hz. Liquid-state NMR spectra were obtained with a 400 MHz Bruker Avance spectrometer (Bruker Biospin, Rheinstetten, Germany), equipped with a 5 mm Bruker Inverse Broad Band (BBI) probe, working at ^{1}H and ^{13}C frequencies of 400.13 and 100.62.

The ^{31}P NMR spectra of CTMP-derivatized Ox extracts were acquired by applying an inverse gated pulse sequence including a 80 μs length (15.6 dB power level) Waltz16 scheme to decouple phosphorus from proton nuclei. In particular, spectra consisted in a 45° pulse length of 5.25 μs, a spectral width of 400 ppm (64 935.066 Hz), 10 s of recycle delay, 1600 transients, 8 dummy scans, and 129 862 time domain points.

^{1}H DOSY (diffusion ordered spectroscopy) NMR experiments were conducted by dissolving 10.0 mg of water-soluble extacts in 1.0 mL of deuterated dimethyl sulfoxide, and applying a stimulated echo pulse sequence with bipolar gradients, combined with two spoil gradients and an eddy current delay, in order to reduce the loss of signals due to short spin—spin relaxation times. The acquisition was conducted by setting 1400 μs long sine-shaped gradients (δ), that linearly ranged from 0.674 to 32.030 G cm^{-1} in 32 increments, and selecting a diffusion delay of 0.1 s (Δ) between encoding and decoding gradients. DOSY experiments consisted in a recycle delay of 2 s, 4096 points, a spectral width of 14 ppm (5592.8 Hz), 64 scans, and 4 dummy scans. The Fourier transform of FIDs was conducted by applying a 2-fold zero filling in the F2 dimension and multiplying by a 2 Hz exponential function.

All NMR spectra were acquired at a temperature of 298 ± 1 K and processed by using either Bruker Topspin Software (v.2.1, Bruker Biospin, Rheinstetten, Germany) or MestReC NMR Processing Software (v.4.8.6.0, Cambridgesoft, Cambridge, Massachusetts, USA). Zero filling was applied during Fourier transform of FIDs.

High Performance Size Exclusion Chromatography (HPSEC). The HPSEC system consisted of a Shimadzu LC-10-AD pump equipped with a Rheodyne rotary injector and 100-μL sample loop and a UV—vis detector (Perkin e Elmer LC295), set at 280 nm. The chromatographic column was a PolySep GFC-P3000 300 × 7.80 mm (Phenomenex, USA), preceded by a PolySep GFC-P 35 × 7.80 safety guard (Phenomenex, USA) and a 2 mm inlet filter. The elution flow rate was set to 0.6 mL min^{-1}, while the eluting solution was made of 0.1 mol L^{-1} NaH_2PO_4 solution buffered at pH 6.5 and 4.6 mmol L^{-1} NaN_3. The eluent solution was also used to dissolve the Ox-extracts at a concentration of 0.6 g L^{-1}. A second series of similarly prepared sample solutions was added with glacial acetic acid (AcOH) to lower the pH to 3.5 before injection into the HPSEC system. The elution profile before and after AcOH addition is a function of the conformational stability of samples.[16,29] Both mobile phase and Ox-BYP solutions were filtered through 0.45 μm Millipore filter prior to the chromatographic analyses. The column calibration was obtained with the following sodium polystyrenesulfonates of known molecular masses: 123 000, 16 900, and 6780 Da. Ferulic acid (194 Da) and catechol (110 Da) were used as low molecular weight standards. The calibration curves provided the following relations between molecular weight (MW) and retention time (RT):

$$\log \mathrm{Mw} = 0.1407RT + 6.4077 \quad (R^2 = 0.9962) \tag{1}$$

DOI: 10.1021/acssuschemeng.7b01928
ACS Sustainable Chem. Eng. XXXX, XXX, XXX—XXX

Weight-averaged (Mw) and number-averaged (Mn) molecular weights and polydispersity (P = Mw/Mn) were calculated as described elsewhere.[30] A Unipoint Gilson Software was used to record and elaborate the chromatograms, while the calculations of Mw, Mn, and P have been performed with the Origin software (v. 9.1, Originlab).

Germination of Maize Seeds and Seedling Emergence. Maize (*Zea mays* L. cv Aapotheoz Limagrain) seeds were soaked in tap water overnight and 15 seeds were placed for each replicate on round filter paper placed in a Petri dish. The experiment was run in five replicates. The filters were moistened with 15 mL of aqueous solution of lignin Ox-extracts at a concentration of 0, 1, 10, and 100 mg of organic carbon L^{-1} (ppm of OC). Seeds were germinated in the dark at 25 °C for 96 h and, thereafter, lengths of coleoptile, radicle, and lateral seminal roots were measured.

As for the growth experiment, maize (cv Aapotheoz Limagrain) seeds were germinated in the dark at 25 °C for 5 days and the seedlings (15 for each treatment) were then placed in plastic test-tubes, and added with 18 mL of a modified Hoagland solution[31] composed as it follows: 40 μM KH_2PO_4, 200 μM $Ca(NO_3)_2$, 200 μM KNO_3, 200 μM $MgSO_4$, 10 μM FeNaEDTA, 4.6 μM H_3BO_3, 0.036 μM $CuCl_2{\cdot}2H_2O$, 0.9 μM $MnCl_2{\cdot}4H_2O$, 0.09 μM $ZnCl_2$, 0.01 μM $NaMoO_3{\cdot}2H_2O$. Tubes with seedlings were placed in a climate chamber that maintained 16 h of light per day, air temperature at 24 °C, and relative humidity at 50%. After 7 days from transplanting, 18 mL of either Ox-BYP 1 or 2 solutions at the organic carbon concentrations of 0 (control), 1, 10, and 100 mg C L^{-1} (ppm of OC) were added to the growing seedlings. After 96 h, plants were harvested and the fresh and dry weights for shoots and roots, and root lengths were determined. Seedling and plantlet roots from both germination and growth experiments were scanned with an Epson Perfection V700 modified flatbed scanner, while length measurements were obtained by using the WinRhizo software, version 2012b (Regent Instruments, Inc.).

Statistical Analysis. All measurements were normally distributed, according the Shapiro–Wilk test ($p < 0.05$), and the one-way ANOVA and post hoc Tukey's range tests were used to compare means among treatments ($p < 0.05$). All statistical elaboration was conducted using SPSS, version 21 (IBM SPPS Statistics).

RESULTS

Elemental Analysis. Both BYP materials showed similar elemental composition (Table 1), and so did the two oxidized extracts, while both carbon and oxygen were larger in BYP than in Ox-BYP materials. This can be accounted to the oxidative extraction undergone by the BYP materials that may have promoted the loss of carbon dioxide or simple organic oxygenated molecules by either volatilization or dialysis.[32]

Table 1. Relative Amount (%) of Carbon (C), Nitrogen (N), Hygrogen (H), and Oxygen (O) on a Dry Ash-Free Basis in the Biorefinery-Derived Materials before (BYP 1 and 2) and after (Ox-BYP 1 and 2) the Alkaline Oxidative Treatment

substrate	C	N	H	O
BYP 1	48.1	1.0	5.6	45.3
BYP 2	48.7	1.0	5.5	44.9
Ox-BYP 1	43.2	1.3	4.9	50.6
Ox-BYP 2	45.9	1.5	4.8	47.9

^{13}C CPMAS NMR Spectroscopy. The ^{13}C CPMAS spectra of the four residues are shown in Figure 1, while signal attribution and relative carbon distribution over different chemical shift regions are reported in Table 2. The signals within the 0–45 ppm range were attributed to alkyl carbons, while the resonance around 56 ppm was assigned to lignin methoxyl groups.[33] The chemical shift interval between 60 and 90 ppm contained the resonances of hydroxylated carbons in either residual cell wall carbohydrates or lignin lateral chains, while anomeric carbons in sugars were in the 90–110 ppm range.[34,35] Aromatic and phenolic carbons resonated in the 110–160 ppm interval, while signals of carboxyl carbons were found between 160 and 190 ppm.[36]

The two lignocellulosic biorefinery residues showed significant different amounts of alkyl and aromatic/phenolic moieties, being the alkyl carbon twice larger in BYP 1 than in BYP 2, and, instead, the aromatic carbon much greater in BYP 2 (Table 2). Such different composition should be ascribed to the diverse treatments undergone by the GR biomass. In fact, it appears that buffering the cellulose-hydrolytic solution for BYP 1 with a larger amount of sodium acetate and extending the extraction time, resulted in a less efficient cleavage of the alkyl components and larger separation of aromatic compounds. In addition, this buffering method led to a slightly smaller amount of carbohydrate signals (Table 2), thus indicating a more efficient cellulose separation during this biomass pretreatment.

Both Ox-BYP samples showed a comparable carbon distribution, though significantly different from that of the original materials (Table 2). As expected, the Ox-BYP extracts was far richer in carboxyl carbon than the starting materials (Table 2). This is in line with previous findings where an increase in acidity was reported, since treatment of lignocellulosic biomasses with alkaline H_2O_2 promoted the oxidative ring-opening in Dakin-like reactions and the oxidation of primary alcohols and aldehydes.[32,37] Furthermore, the relative content of anomeric carbon (Table 2) suggests that some plant carbohydrates still remained in oxidized samples, though significantly less than in the starting BYP residues.

^{31}P NMR Spectroscopy. The 2-chloro-4,4,5,5-tetramethyl-1,3,2-dioxa-phospholane (CTMP) is a ^{31}P-derivatizating reagent that allows to quantify acidic functional groups in lignin and lignin-like materials. The liquid-state ^{31}P NMR spectra of CTMP-derivatized samples reveal enhanced intensity of ^{31}P NMR signals and their spreading over a large spectral width.[38] The type and amount of ^{31}P-derivatized OH groups in Ox-BYP 1 and 2 are reported in Figure 2 and in Table 3, respectively. The resonance of alcoholic groups is located between 150.8 and 146.3 ppm, while the phenolic and carboxyl moieties are found in the 143.7–142.2 and 135.6–133.7 ppm ranges, respectively.[39] While the aliphatic OH content was similar in both Ox-extracts, the amount of various phenolic OH groups, such as syringyl (S), condensed phenolic (CP), guaiacyl, and *p*-hydroxyphenyl groups, were larger in Ox-BYP 2 than in Ox-BYP 1 (Table 3). This finding, coupled with the significant lower amount of carboxyl groups (about 18% less than in Ox-BYP 1), suggests a more hydrophobic nature of Ox-BYP 2 (Table 3).

The different phenolic content in the two materials is primarily due to the amount of S and CP molecules. The significantly diverse content of S-derived molecules (about 47% more in Ox-BYP 2) is likely due to the different hydrolyzing treatments undergone by the GR residual biomass, that presumably made the S compounds in BYP 1 more prone to degradation during the subsequent alkaline extraction. The reported large reactivity of S molecules in the H_2O_2 alkaline solutions[40,41] may have then caused the greater loss of such compounds while extracting Ox-BYP 1. Moreover, this explanation is further corroborated by the 39% larger content of condensed phenolics in Ox-BYP 2 than in Ox-BYP 1, thus suggesting that the hydrolysis of the GR biomass residue with a less concentrated buffer (as for BYP 2) reduced the reactivity of

DOI: 10.1021/acssuschemeng.7b01928
ACS Sustainable Chem. Eng. XXXX, XXX, XXX–XXX

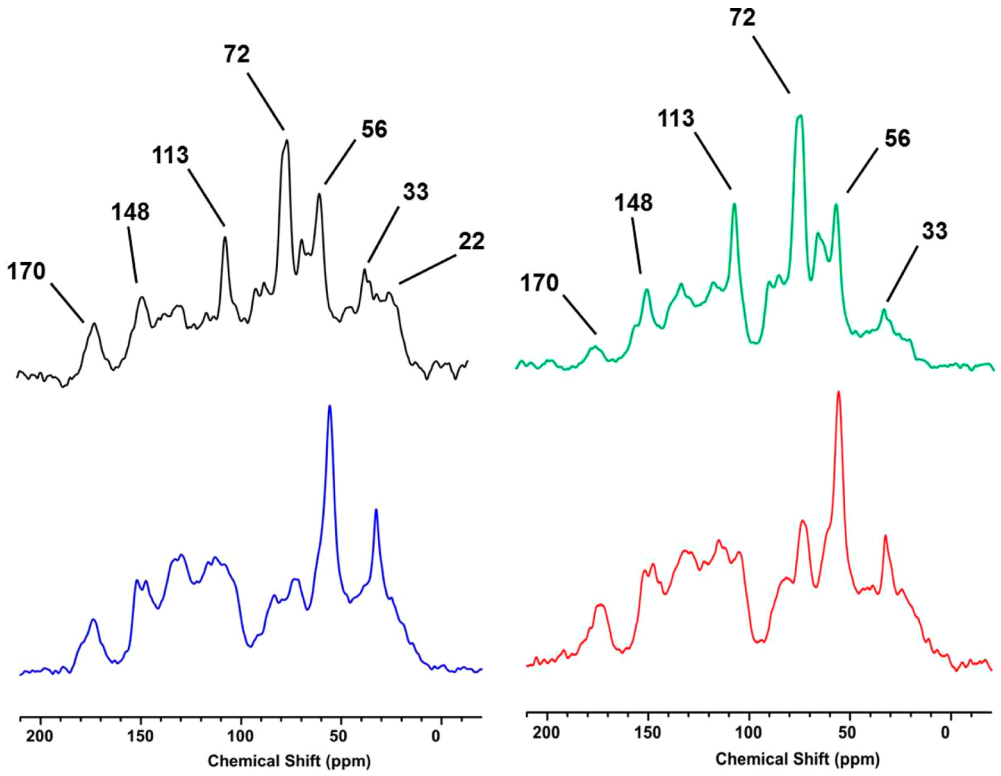

Figure 1. ^{13}C CPMAS NMR spectra for hydrolyzed lignocellulosic residues (BYP 1 black line and BYP 2 green line) and their alkaline extracts (Ox-BYP 1 blue line and Ox-BYP 2 red line).

Table 2. Relative Carbon Distribution (%) in Chemical Shift Regions (ppm) of ^{13}C CPMAS NMR Spectra of Hydrolyzed Biorefinery Wastes before (BYP 1 and 2) and after (Ox-BYP 1 and 2) the Alkaline Oxidative Extraction

chemical shift range (ppm)	attribution	BYP 1	BYP 2	Ox-BYP 1	Ox-BYP 2
0–45	alkyl C	20.55	10.22	19.66	17.39
45–60	methoxyl C	12.61	11.53	16.04	15.62
60–90	hydroxyl-bearing C	30.78	35.26	17.94	20.55
90–110	anomeric C	12.29	12.75	9.39	8.62
110–145	aryl C	16.93	21.93	24.64	24.47
145–160	*O*-aryl C	3.97	5.69	7.67	7.57
160–190	carboxyl	2.87	2.62	4.66	5.78

phenolic compounds in the following alkaline oxidative extraction (Table 3). Alternatively, the different enzymatic hydrolyses may have varied the availability of phenolic moieties from the two lignocellulosic matrices to the H_2O_2 extraction, thus resulting in different chemical properties.

Water-soluble lignins from raw giant reed had been previously extracted by the same alkaline procedure employed here and the amount of OH groups were evaluated by ^{31}P NMR after derivatization with CTMP.[14] The S content in the Ox-lignin from the raw untreated plant was markedly larger (370 μmol g^{-1} of lignin) than that found here for the extraction of the hydrolyzed biomass (Table 3). This further indicates that the structure of GR lignin is modified when the biomass undergoes a preliminary steam-explosion and enzymatic hydrolysis, thus making the phenolic molecules more prone to degradation.

^{1}H DOSY NMR Spectroscopy. The DOSY NMR spectroscopy is employed to obtain information on the diffusivity

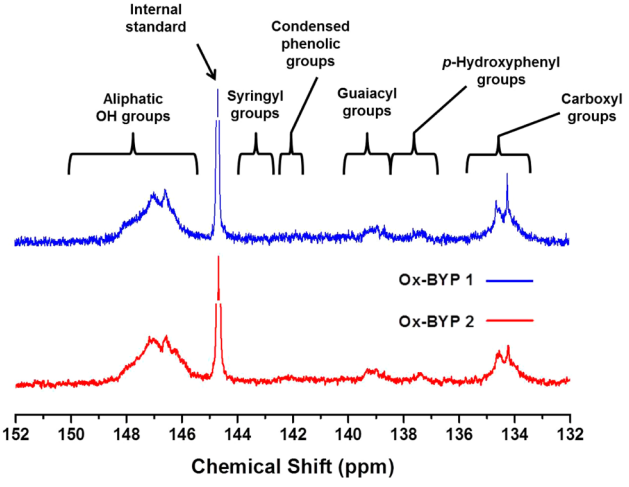

Figure 2. ^{31}P NMR spectra of ^{31}P-derivatized water-soluble materials separated by alkaline extraction from hydrolyzed lignocellulosic residues.

and size of natural organic matter (NOM),[42] since the diffusivity constant of a material is inversely correlated to its molecular mobility and, thus, to its molecular size.[43] The ^{1}H DOSY NMR spectra indicated a smaller overall diffusivity for Ox-BYP 2, and, thus, a larger molecular size than for Ox-BYP 1 (Figure 3). This finding is in line with the significantly greater content of condensed phenolic molecules found for Ox-BYP 2 by ^{31}P NMR spectra (CP in Table 3) and supports the indication that the hydrolysis treatment with a lower amount of buffer provides a residual waste that is less prone to depolymerization during the subsequent alkaline oxidative extraction.

DOI: 10.1021/acssuschemeng.7b01928
ACS Sustainable Chem. Eng. XXXX, XXX, XXX−XXX

Table 3. Structural Assignment, Content (μmol g^{-1} of Lignin) and Percent of Main Compounds Identified in ^{31}P NMR Spectra of Ox-BYP 1 and Ox-BYP 2

chemical shift range (ppm)	assignment	Ox-BYP 1	Ox-BYP 2	Δ (%)[a]
150.8−146.3	aliphatic OH groups	1563.91	1620.24	3.60
143.7−142.2	syringyl groups	43.33	63.46	46.65
142.8−141.7	phenolic OH units in condensed (4−O−5′, 5−5′) lignin dimers	69.07	96.26	39.37
140.2−138.4	guaiacyl groups	276.37	299.46	8.35
138.6−136.9	*p*-hydroxyphenyl groups	131.30	147.53	12.36
135.6−133.7	carboxyl groups	873.73	715.45	−18.12

[a]The Δ value is the percent difference between the values for Ox-BYP 1 and those for Ox-BYP 2, normalized to the Ox-BYP 1 values.

High Performance Size Exclusion Chromatography. The size-exclusion chromatograms of the lignin Ox-extracts before and after acetic acid (AcOH) treatment are shown in Figure 4, while the corresponding weight-averaged (Mw), number-averaged (Mn) molecular weights, and polydispersity (*P*) values are reported in Table 4. The two Ox-extracts revealed comparable profiles, with two absorption peaks at same elution intervals (Figure 4), as well as very similar Mw and Mn (Table 4). The solutions of the Ox-extracts were then added with AcOH to bring the pH from 6.5 down to 3.5 and another elution profile was recorded for both Ox-BYP 1 and Ox-BYP 2 (Figure 4). This method had been previously adopted to study the strength of association of humic (HS) and humic-like substances (HULIS) composed of relatively low molecular weight compounds arranged in suprastructures, which are stabilized only by weak, dispersive intermolecular forces (van der Waals, $\pi-\pi$, π−CH) and/or hydrogen bonds.[44] The loosely bound supramolecular assemblies can be disrupted into smaller associations by very little amount of AcOH, because of the formation of intra- and intermolecular hydrogen bonds that are stronger than the weak dispersive forces stabilizing the superstructure at pH 6.5.[29] This significant change in conformation upon AcOH addition is typical of supramolecular structures, whereas covalently linked polymers are by no means affected. The evaluation of changes in HPSEC elution profiles before and after the AcOH treatment represents a valuable tool to assess whether a complex mixture displays a supramolecular or a polymeric nature.[29,45]

The AcOH addition to the Ox-extracts resulted in a substantial modification in the conformational arrangement of Ox-BYP 1, whereas only slight changes were noted in the HPSEC chromatogram of Ox-BYP 2 (Figure 4). While both materials appeared to be composed of both a large-size core and unbound small compounds, the more marked change showed by Ox-BYP 1 after AcOH addition suggests that this substrate contained molecules of smaller molecular size than for Ox-BYP 2 (Figure 4; Table 4). The larger hydrodynamic radius observed for Ox-BYP 2 accounts for its notably greater content of condensed phenolic units (Table 3), and it is likely to reflect the poorer hydrolytic efficiency when the ligno-cellulosic biomass was hydrolyzed with a smaller buffer concentration (BYP 2). This inference is well in line with ^{13}C CPMAS , ^{31}P, and ^{1}H DOSY NMR results (Figures 1−3; Tables 2 and 3) and corroborates the hypothesis that the hydrolysis of the lignocellulosic biomass residue is more efficient in more concentrated buffer solutions.

Water-soluble lignin isolated directly from giant reed biomass by the same alkaline oxidative procedure of this work was similarly analyzed by HPSEC before and after AcOH addition.[16] That extract showed a significantly smaller apparent molecular-size distribution even before AcOH addition, thus suggesting the oxidative extraction produced a smaller sized material from raw biomass than from the hydrolyzed residue (Table 4). Nonetheless, the AcOH treatment of that isolate showed a HPSEC profile with an even larger disruption of conformational arrangement, implying a composition of mainly small-sized molecules.[16] Hence, our findings indicate that the alkaline H_2O_2 extraction of lignocellulosic biomasses may provide phenol-rich materials of different hydrodynamic size according to biomass pretreatments.

Germination of Maize Seeds and Emergence of Seedlings. Both the Ox-BYP substrates showed a positive dose-dependent biological activity toward the germination of maize seeds, although the extent of the bioactivity differed with the Ox-extract (Table 5). While Ox-BYP 1 significantly increased the radicle root (RR) length at all the concentrations and up to 17% more than control at the OC concentration of 10 ppm, Ox-BYP 2 promoted a slightly less RR elongation at 10 ppm of OC (10% more than control) and inhibited it at 100 ppm of OC (9% less than control treatment) (Table 5). Also,

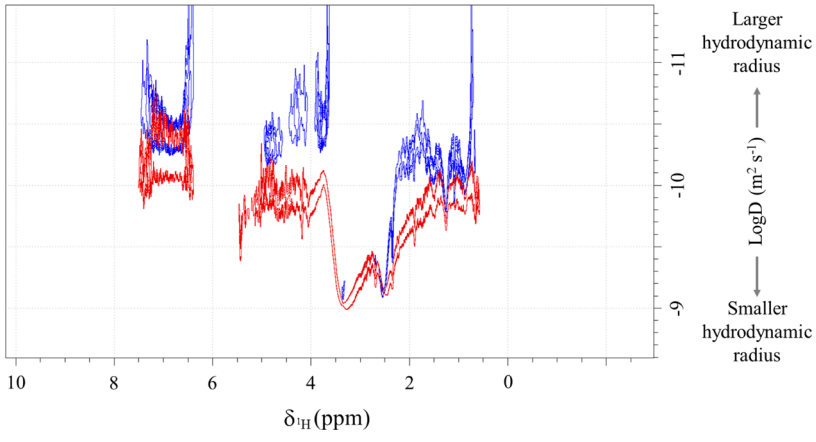

Figure 3. Two-dimensional ^{1}H DOSY NMR projections for water-soluble materials separated by alkaline extraction from hydrolyzed lignocellulosic residues: (blue line) Ox-BYP 1; (red line) Ox-BYP 2.

DOI: 10.1021/acssuschemeng.7b01928
ACS Sustainable Chem. Eng. XXXX, XXX, XXX−XXX

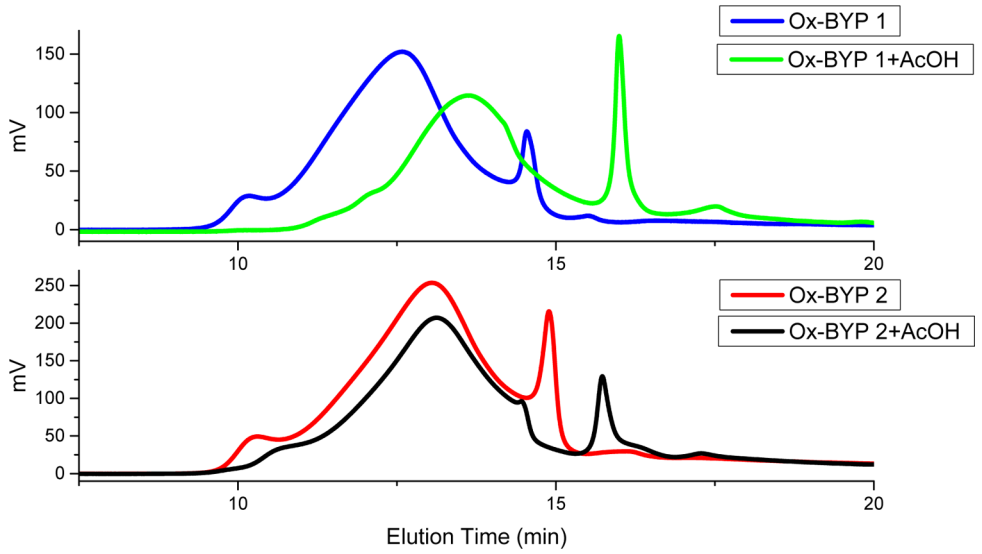

Figure 4. HPSEC of water-soluble Ox-BYP materials before and after addition of acetic acid (AcOH) to adjust the mobile phase from 7 to pH 3.5.

Table 4. Weight Average (Mw) and Number Average (Mn) Molecular Weights and Polydispersity (*P*) at Different Elution Time Intervals (min) in UV-Detected HPSEC Chromatograms for Ox-BYP 1 and Ox-BYP 2 Samples before and after Addition of Acetic Acid

elution interval (min)	sample	Mw	Mn	*P*
8.9–14.3	Ox-BYP 1 (peak A)	42812	38751	1.1
14.3–15.9	(peak B)	18656	18333	1.0
9.4–15.6	Ox-BYP 1 + AcOH (peak A)	29496	27078	1.1
15.6–16.6	(peak B)	12814	12756	1.0
16.6–18.8	(peak C)	7901	7656	1.0
9.0–14.5	Ox-BYP 2 (peak A)	40960	36336	1.1
14.5–15.6	(peak B)	20982	20807	1.0
9.0–15.3	Ox-BYP 2 + AcOH (peak A)	38278	34026	1.0
15.3–16.9	(peak B)	17504	17394	1.0

Table 5. Length (cm) of Radicle Root, Lateral Seminal Root, and Coleoptile for Maize Seedlings Treated with Aqueous Solutions (ppm of Organic Carbon) of Ox-BYP 1 and Ox-BYP 2[a]

		treatment (ppm)		
	biorefinery-derived substrate	0	10	100
radicle	Ox-BYP 1	6.58 (100)^{a}	7.57 (117)^{b}	6.83 (106)^{ab}
	Ox-BYP 2	5.59 (100)^{ab}	6.13 (110)^{b}	5.09 (91)^{a}
LSR	Ox-BYP 1	9.45 (100)^{a}	10.56 (111)^{b}	9.3 (98)^{a}
	Ox-BYP 2	7.32 (100)^{a}	10.33 (141)^{c}	9.58 (131)^{b}
coleoptile	Ox-BYP 1	4.70 (100)^{a}	4.94 (105)^{a}	5.17 (110)^{b}
	Ox-BYP 2	5.68 (100)^{a}	6.45 (114)^{b}	5.71 (101)^{a}

[a]Values in parentheses refer to raw data normalized to control values set at 100. Different letters in rows indicate significant differences at 0.05 probability level, as revealed by the Tukey's test

the lateral seminal root (LSR) length was influenced by the Ox-treatments to different extents. In particular, Ox-BYP 1 enhanced the LSR elongation only at 10 ppm of OC (11% more than control), whereas Ox-BYP 2 stimulated LSR development at both 10 and 100 ppm of OC, with a 41 and 31% increase more than control, respectively (Table 5). As for the coleoptile development, a slight increase at larger concentrations was noted for Ox-BYP 1, while Ox-BYP 2 resulted in bioactivity only at 10 ppm of OC (14% more than control) (Table 5).

Both Ox-extracts displayed a positive bioactivity toward maize germination, especially at 10 ppm of OC (Table 6). The application of these substrates may have induced a modification of the internal seeds hormonal balance, thus prompting their germination. In fact, it has been already reported that phenolic molecules may exert a gibberellin (GA) like activity toward plant development.[20,46] Also water-soluble lignins isolated from raw giant reed by the same alkaline oxidative procedure employed here had shown a significant dose-dependent gibberellin activity.[47] In particular, the abscisic acid (ABA) to GA ratio (ABA/GA) appears to govern the germination process, while ABA promotes seed dormancy, and GA is involved in breaking seed dormancy and initiating seed germination.[48] Hence, a large ABA/GA ratio is related to the preservation of seed dormancy, whereas a small ABA/GA ratio prompts germination.[48] Both phenolic molecules and phenol-rich substrates were previously shown to affect this balance, by reducing the inhibitory effect of ABA and, hence, stimulating seed germination.[49−51] Our results seem thus to indicate that the Ox-extracts from the buffered-treated biomass may alter the metabolic pathways of maize seed germination and induce a faster plant protrusion.

The Ox-BYP extracts have been also assayed for their biostimulant properties toward growth of maize plantlets by measuring several phenological parameters (Table 6). The total fresh weight (TFW) of maize seedlings was inhibited by Ox-BYP 1 at 1 ppm of OC, whereas it was significantly increased at 100 ppm of OC in respect to control. A similar plant growth was observed when 1 ppm of OC of Ox-BYP 2 was used, while this material resulted ineffective in comparison to control at 10 and 100 ppm of OC (Table 6). Comparable results were observed for root fresh weight (RFW) which was negatively affected by Ox-BYP 1 at 1 ppm of OC, while a significant increase (8% more than control) was noted when the maize seedling was added with 100 ppm of OC of the same extract.

DOI: 10.1021/acssuschemeng.7b01928
ACS Sustainable Chem. Eng. XXXX, XXX, XXX−XXX

Table 6. Total Fresh Weight (TFW, g), Root Fresh Weight (RFW, g), Shoot Fresh Weight (SFW, g), Total Dry Weight (TDW, g), Root Dry Weight (RDW, g), Shoot Dry Weight (SDW, g), and Root Length (RL, cm) for Maize Seedlings Treated with Different Concentrations of Aqueous Solutions (ppm of Organic Carbon) of Ox-BYP 1 and Ox-BYP 2[a]

		Ox-BYP 1			Ox-BYP 2		
	control	1	10	100	1	10	100
TFW	1.541 (100)^{ab}	1.481 (96)^{a}	1.550 (101)^{ab}	1.647 (107)^{c}	1.615 (105)^{bc}	1.575 (102)^{ab}	1.554 (101)^{ab}
RFW	0.996 (100)^{ab}	0.958 (96)^{a}	0.990 (99)^{ab}	1.073 (108)^{c}	1.045 (105)^{bc}	1.002 (101)^{ab}	1.004 (101)^{ab}
SFW	0.545 (100)^{a}	0.523 (95)^{a}	0.560 (103)^{ab}	0.55 (101)^{a}	0.570 (105)^{b}	0.573 (105)^{b}	0.573 (105)^{b}
TDW	0.219 (100)^{ab}	0.209 (95)^{a}	0.214 (98)^{ab}	0.246 (112)^{c}	0.256 (117)^{c}	0.225 (103)^{b}	0.232 (106)^{b}
RDW	0.178 (100)^{ab}	0.170 (95)^{a}	0.191 (107)^{bc}	0.202 (113)^{c}	0.212 (119)^{c}	0.183 (103)^{b}	0.189 (106)^{b}
SDW	0.041 (100)^{a}	0.039 (96)^{a}	0.043 (104)^{ab}	0.044 (107)^{b}	0.044 (107)^{b}	0.042 (103)^{ab}	0.042 (103)^{ab}
RL	97.475 (100)^{ab}	90.417 (93)^{a}	96.480 (99)^{ab}	107.918 (111)^{b}	87.030 (89)^{a}	97.450 (100)^{ab}	92.278 (95)^{ab}

[a]Values in parentheses refer to raw data normalized to control values set at 100. Different letters in rows indicate significant differences at 0.05 probability level, as revealed by the Tukey's test.

Conversely, only the 1 ppm of OC solution of Ox-BYP 2 showed a significant positive bioactivity on RFW with respect to control (Table 6). In the case of the measurement of shoot fresh weight (SFW) Ox-BYP 1 provided a significant bioactivity only at 100 ppm of OC, whereas Ox-BYP 2 similarly affected maize SFW at any tested concentrations (Table 6). The total dry weight (TDW) was reduced by 1 ppm of OC of Ox-BYP 1, while it was comparable to control for the 10 ppm of OC application and significantly larger (12%) than control for the 100 ppm of OC concentration. Conversely, Ox-BYP 2 increased TDW over control at any assayed concentration, with the maximum stimulation found at 1 ppm of OC (17% larger than control) (Table 6).

A significant bioactivity related to root dry weight (RDW) was recorded for both Ox-extracts at all tested concentrations, except for the 1 ppm of OC concentration of Ox-BYP 1. In particular, the maximum bioactive effect on RDW was shown, in the order, at 100 and 1 ppm of OC for both Ox-BYP 1 and 2, which determined a RDW increase of 13 and 19% more than control, respectively (Table 6). The increase of shoot dry weight (SDW) was statistically significant at 10 and 100 ppm of OC for Ox-BYP1, whereas Ox-BYP 2 determined a SDW increase at all tested concentrations, with the maximum effect at 1 ppm of OC (7% more than control) (Table 6). As for root length (RL), a positive bioactivity was found only by applying Ox-BYP 1 at a concentration of 100 ppm of OC, that determined an increase of root length of 11% larger than control (Table 6; Supporting Figure 1).

The plant growth experiments showed that application of Ox-BYP 1 resulted in a general increasingly positive bioactivity at 10 and 100 ppm of OC, while the 1 ppm of OC solution repressed the development of maize plantlets (Table 6). This negative effect at 1 ppm of OC suggests that Ox-BYP 1 may contain inhibitory compounds, that are likely to be released when this Ox-extract interacts with the root surface. Here, we can infer that plant root-extruded protons determine a disruption of the Ox-BYP 1 conformational structure inasmuch as that observed by the AcOH treatment in the HPSEC experiment, with the consequent possible release of plant noxious molecules. On the contrary, the Ox-BYP 1 molecules may associate in larger clusters at greater concentrations (10 and 100 ppm of OC), whose conformational stability is strong enough to resist the disruption by the root-exuded protons. Hence, the growth inhibition is overcome at larger concentrations, that are even positively bioactive on plant growth.

The positive influence displayed by Ox-BYP 2 may be also related to a stable conformation due to its significantly greater hydrophobicity than Ox-BYP 1. These physical–chemical properties may determine a strong adsorption onto the root surface, thus allowing a closer interaction with root cells and the stimulation of plant growth processes.[17] In fact, the addition of 100 ppm of OC of Ox-BYP 1 and 1 ppm of OC of Ox-BYP 2 similarly affects the plant total and root fresh weight, as well as the total, root, and shoot dry weight (Table 6), thereby suggesting that similar mechanisms of plant biostimulation occur for the two Ox-extracts, but at different concentrations.

CONCLUSIONS

Water-soluble lignins separated from biorefinery wastes were shown here to promote the germination and growth of maize seeds and seedlings. We indicated that this bioactivity depended on both the applied concentration and the molecular properties of extracts. Ox-BYP 2 increased plant development even at small doses, whereas Ox-BYP 1 was effective only at larger concentrations. The Ox-BYP 2 hydrophobic composition enhanced bioactivity due to its adhesion to roots, while biostimulation of the loosely bound Ox-BYP 1 was triggered by the release of bioactive compounds upon interaction with root exudates. Both extracts from hydrolyzed lignocellulosic wastes were shown to be bioactive on plants, and they promise to become useful sustainable biostimulants of crop growth.

ASSOCIATED CONTENT

Supporting Information

The Supporting Information is available free of charge on the ACS Publications website at DOI: 10.1021/acssuschemeng.7b01928.

Scans of maize roots treated with different concentrations of aqueous solutions of Ox-BYP 1 and Ox-BYP 2 (PDF)

AUTHOR INFORMATION

Corresponding Authors

*E-mail: alessandro.piccolo@unina.it (A.P.).
*E-mail: davide.savy@unina.it (D.S.).

ORCID

Marios Drosos: 0000-0003-0403-7014
Vincenza Cozzolino: 0000-0002-5618-254X

Notes

The authors declare no competing financial interest.

DOI: 10.1021/acssuschemeng.7b01928
ACS Sustainable Chem. Eng. XXXX, XXX, XXX−XXX

■ ACKNOWLEDGMENTS

This work was funded by the MIUR project PON03PE_00107_01 "BioPoliS".

■ REFERENCES

(1) Jayawardena, D. M.; Heckathorn, S. A.; Bista, D. R.; Mishra, S.; Boldt, J. K.; Krause, C. R. Elevated CO_2 plus chronic warming reduce nitrogen uptake and levels or activities of nitrogen-uptake and -assimilatory proteins in tomato roots. *Physiol. Plant.* **2017**, *159*, 354−365.

(2) Kundu, A.; Sahu, J. N.; Redzwan, G.; Hashim, M. An overview of cathode material and catalysts suitable for generating hydrogen in microbial electrolysis cell. *Int. J. Hydrogen Energy* **2013**, *38*, 1745−57.

(3) Vohra, M.; Manwar, J.; Manmode, R.; Padgilwar, S.; Patil, S. Bioethanol production: feedstock and current technologies. *J. Environ. Chem. Eng.* **2014**, *2*, 573−84.

(4) Searle, S. Y.; Malins, C. J. Waste and residue availability for advanced biofuel production in EU Member States. *Biomass Bioenergy* **2016**, *89*, 2−10.

(5) Lin, C. S. K.; Pfaltzgraff, L. A.; Herrero-Davila, L.; Mubofu, E. B.; Abderrahim, S.; Clark, J. H.; Koutinas, A.; Kopsahelis, N.; Stamatelatou, K.; Dickson, F.; Thankappan, S.; Mohamed, Z.; Brocklesby, R.; Luque, R. Food waste as a valuable resource for the production of chemicals, materials and fuels. Current situation and global perspective. *Energy Environ. Sci.* **2013**, *6*, 426−464.

(6) Cherubini, F. The biorefinery concept: using biomass instead of oil for producing energy and chemicals. *Energy Convers. Manage.* **2010**, *51*, 1412−1421.

(7) Ma, Y.; Yin, Y.; Liu, Y. A holistic approach for food waste management towards zero-solid disposal and energy/resource recovery. *Bioresour. Technol.* **2017**, *228*, 56−61.

(8) Vishtal, A.; Kraslawski, A. Challenges in industrial applications of technical lignins. *Bioresources* **2011**, *6*, 3547−3568.

(9) Doherty, W. O. S; Mousavioun, P.; Fellows, C. M. Value-adding to cellulosic ethanol: Lignin polymers. *Ind. Crops Prod.* **2011**, *33*, 259−276.

(10) Domínguez-Robles, J.; Espinosa, E.; Savy, D.; Rosal, A.; Rodríguez, A. Biorefinery process combining Specel® process and selective lignin precipitation using mineral acids. *BioResources* **2016**, *11*, 7061−7077.

(11) Octave, S.; Thomas, D. Biorefinery: Toward an industrial metabolism. *Biochimie* **2009**, *91*, 659−664.

(12) Popa, V. I.; Dumitru, M.; Volf, I.; Anghel, N. Lignin and polyphenols as allelochemicals. *Ind. Crops Prod.* **2008**, *27*, 144−149.

(13) Savy, D.; Cozzolino, V.; Vinci, G.; Nebbioso, A.; Piccolo, A. Water-Soluble Lignins from Different Bioenergy Crops Stimulate the Early Development of Maize (*Zea mays*, L.). *Molecules* **2015**, *20*, 19958−19970.

(14) Savy, D.; Mazzei, P.; Drosos, M.; Nebbioso, A.; Piccolo, A. Molecular composition of water-soluble lignins separated from different *non*-food biomasses. *Fuel Process. Technol.* **2015**, *131*, 175−181.

(15) Chakar, F. S.; Ragauskas, A. J. Review of current and future softwood kraft lignin process chemistry. *Ind. Crops Prod.* **2004**, *20*, 131−141.

(16) Savy, D.; Cozzolino, V.; Nebbioso, A.; Drosos, M.; Nuzzo, A.; Mazzei, P.; Piccolo, A. Humic-like bioactivity on emergence and early growth of maize (*Zea mays* L.) of water-soluble lignins isolated from biomass for energy. *Plant Soil* **2016**, *402*, 221−233.

(17) Canellas, L. P.; Olivares, F. L. Physiological responses to humic substances as plant growth promoter. *Chem. Biol. Technol. Agric.* **2014**, *1*, 3.

(18) Monda, H.; Cozzolino, V.; Vinci, G.; Spaccini, R.; Piccolo, A. Molecular characteristics of water-extractable organic matter from different composted biomasses and their effects on seed germination and early growth of maize. *Sci. Total Environ.* **2017**, *590*−*591*, 40−49.

(19) Aremu, A. O.; Masondo, N. A.; Rengasamy, K. R.; Amoo, S. O.; Gruz, J.; Bíba, O.; Šubrtová, M.; Pěnčík, A.; Novák, O.; Doležal, K.; Van Staden, J. Physiological role of phenolic biostimulants isolated from brown seaweed *Ecklonia maxima* on plant growth and development. *Planta* **2015**, *241*, 1313−1324.

(20) Ertani, A.; Schiavon, M.; Altissimo, A.; Franceschi, C.; Nardi, S. Phenol-containing organic substances stimulate phenylpropanoid metabolism in *Zea mays*. *J. Plant Nutr. Soil Sci.* **2011**, *174*, 496−503.

(21) Saa, S.; Olivos-Del Rio, A.; Castro, S.; Brown, P. H. Foliar application of microbial and plant based biostimulants increases growth and potassium uptake in almond (*Prunus dulcis* (Mill.) D. A. Webb). *Fron. Front. Plant Sci.* **2015**, *6*, 1−9.

(22) Angelini, L. G.; Ceccarini, L.; Nassi o di Nasso, N.; Bonari, E. Comparison of *Arundo donax* L. and *Miscanthus x giganteus* in a long-term field experiment in Central Italy: analysis of productive characteristics and energy balance. *Biomass Bioenergy* **2009**, *33*, 635−643.

(23) Lewandowski, I.; Scurlock, J. M.; Lindvall, E.; Christou, M. The development and current status of perennial rhizomatous grasses as energy crops in the US and Europe. *Biomass Bioenergy* **2003**, *25*, 335−361.

(24) Garbero, M.; Ottonello, P.; Cotti, C. M.; Ferrero, S.; Torre, P.; Cherchi, F.; Bonanni, A. Improved biomass pretreatment process. PatentNo WO 2010113129:A3, 2010.

(25) De Bari, I.; Liuzzi, F.; Villone, A.; Braccio, G. Hydrolysis of concentrated suspensions of steam pretreated *Arundo donax*. *Appl. Energy* **2013**, *102*, 179−189.

(26) Cimini, D.; Argenzio, O.; D'Ambrosio, S.; Lama, L.; Finore, I.; Finamore, R.; Pepe, O.; Faraco, V.; Schiraldi, C. Production of succinic acid from *Basfia succiniciproducens* up to the pilot scale from *Arundo donax* hydrolysate. *Bioresour. Technol.* **2016**, *222*, 355−360.

(27) ASTM E1755-01 Standard Method for the Determination of Ash in Biomass. In *Annual Book of ASTM Standards*; American Society for Testing and Materials, International: Philadelphia, PA, 2003, Vol. *11.05*.

(28) Hatzakis, E.; Dagounakis, G.; Dais, P.; Agiomyrgianaki, A. A Facile NMR method for the quantification of total free and esterified sterols in virgin olive oil. *Food Chem.* **2010**, *122*, 346−352.

(29) Piccolo, A. The Supramolecular structure of humic substances. A novel understanding of humus chemistry and implications in soil Science. *Adv. Agron.* **2002**, *75*, 57−134.

(30) Striegel, A.; Yau, W. W.; Kirkland, J. J.; Bly, D. D. *Modern size exclusion chromatography* **2009**, 193.

(31) Hoagland, D. R.; Arnon, D. I. *The water culture method for growing plants without soil*, California Agricultural Experimental Station Circular No. 347; University of California: Berkeley, 1950; pp 1−32.

(32) Kadla, J. K.; Chang, H.; Jameel, H. The reactions of lignins with hydrogen peroxide at high temperature. Part 2.The oxidation of kraft lignin. *Holzforschung* **1999**, *53*, 277−284.

(33) Savy, D.; Piccolo, A. Physical-chemical characteristics of lignins separated from biomasses for second-generation ethanol. *Biomass Bioenergy* **2014**, *62*, 58−67.

(34) Husson, E.; Buchoux, S.; Avondo, C.; Cailleu, D.; Djellab, K.; Gosselin, I.; Wattraint, O.; Sarazin, C. Enzymatic hydrolysis of ionic liquid-pretreated celluloses: Contribution of CP-MAS 13C NMR and SEM. *Bioresour. Technol.* **2011**, *102*, 7335−7342.

(35) Savy, D.; Mazzei, P.; Roque, R.; Nuzzo, A.; Bowra, S.; Santos, R. Structural recognition of lignin isolated from bioenergy crops by subcritical water:ethanol extraction. *Fuel Process. Technol.* **2015**, *138*, 637−644.

(36) Domínguez-Robles, J.; Sánchez, R.; Espinosa, E.; Savy, D.; Mazzei, P.; Piccolo, A.; Rodríguez, A. Isolation and Characterization of Gramineae and Fabaceae Soda Lignins. *Int. J. Mol. Sci.* **2017**, *18*, 327.

(37) Dakin, H. D. The oxidation of hydroxy derivatives of benzaldehyde, acetophenone and related substances. *Am. Chem. J.* **1909**, *42*, 477−498.

(38) Argyropoulos, D. S. Heteronuclear NMR Spectroscopy of Lignins. In *Lignin and Lignans: Advances in Chemistry*; Heitner, C., Dimmel, D. R., Schmidt, J. A., Eds.; Taylor and Francis Group, LLC: Boca Raton, FL, 2010.

DOI: 10.1021/acssuschemeng.7b01928
ACS Sustainable Chem. Eng. XXXX, XXX, XXX−XXX

(39) You, T.-T.; Mao, J.-Z.; Yuan, T.-Q.; Wen, J.-L.; Xu, F. Structural elucidation of the lignins from stems and foliage of *Arundo donax* Linn. *J. Agric. Food Chem.* **2013**, *61*, 5361−5370.
(40) Sultanov, V.; Wallis, A. Reactivities of guaiacyl and syringyl lignin model phenols towards oxidation with oxygen-alkali. *J. Wood Chem. Technol.* **1991**, *11*, 291−305.
(41) Tsutsumi, Y.; Kondo, R.; Sakai, K.; Imamura, H. The difference of reactivity between syringyl lignin and guaiacyl lignin in alkaline systems. *Holzforschung* **1995**, *49*, 423−428.
(42) Nebbioso, A.; Mazzei, P.; Savy, D. Reduced complexity of multidimensional and diffusion NMR spectra of soil humic fractions as simplified by humeomics. *Chem. Biol. Technol. Agric.* **2014**, *1*, 24.
(43) Johnson, C. S., Jr Diffusion ordered nuclear magnetic resonance spectroscopy: principles and applications. *Prog. Nucl. Magn. Reson. Spectrosc.* **1999**, *34*, 203−256.
(44) Piccolo, A.; Conte, P.; Cozzolino, A. Chromatographic and spectrophotometric properties of dissolved humic substances compared with macromolecular polymers. *Soil Sci.* **2001**, *166*, 174−185.
(45) Piccolo, A.; Conte, P.; Cozzolino, A. Effect of mineral and monocarboxylic acids on the molecular association of dissolved humic substances. *Eur. J. Soil Sci.* **1999**, *50*, 687−694.
(46) Ertani, A.; Francioso, O.; Tugnoli, V.; Righi, V.; Nardi, S. Effect of commercial lignosulfonate-humate on *Zea mays* metabolism. *J. Agric. Food Chem.* **2011**, *59*, 11940−11948.
(47) Savy, D.; Canellas, L.; Vinci, G.; Cozzolino, V.; Piccolo, A. Humic-Like Water-Soluble Lignins from Giant Reed (*Arundo donax* L.) Display Hormone-Like Activity on Plant Growth. *J. Plant Growth Regul.* **2017**, 1−7.
(48) Diaz-Vivancos, P.; Barba-Espín, G.; Hernández, J. A. Elucidating hormonal/ROS networks during seed germination: insights and perspectives. *Plant Cell Rep.* **2013**, *32*, 1491−502.
(49) Ray, S. D.; Laloraya, M. M. Interaction of gibberellic acid, abscisic acid, and phenolic compounds in the control of hypocotyl growth of *Amaranthus caudatus* seedlings. *Can. J. Bot.* **1984**, *62*, 2047−2052.
(50) Ray, S. D. GA, ABA, Phenol Interaction in the Control of Growth: Phenolic Compounds as Effective Modulators of GA-ABA Interaction in Radish Seedlings. *Biol. Plant.* **1986**, *28*, 361−369.
(51) Sharma, S.; Sharma, S. S.; Rai, V. K. Reversal by phenolic compounds of abscisic acid-induced inhibition of in vitro activity of amylase from seeds of *Triticum aestivum* L. *New Phytol.* **1986**, *103*, 293.

DOI: 10.1021/acssuschemeng.7b01928
ACS Sustainable Chem. Eng. XXXX, XXX, XXX−XXX